Macedonian Journal of Chemistry and Chemical Engineering, Vol. **44**, No. 2, pp. xx–xx (2025)

MJCCA9 –

ISSN 1857-5552
e-ISSN 1857-5625

Received: October 7, 2025
Accepted: November 13, 2025

DOI: 10.20450/mjcce.2025.3313
Original scientific paper

OPEN-CIRCUIT POTENTIALS IN BIOFILMS: BIOTRANSFORMATION KINETICS GOVERNS THE DYNAMICS UNDER ANAEROBIC CONDITIONS

Ljupcho Pejov[1, 2], Kiril D. Hristovski[1,*], Scott R. Burge[3], Dragan Boscović[4], Frosina Babanovska Milenkovska[5], Russell G. Burge[3]

[1]*Environmental and Resource Management Program, The Polytechnic School, Ira A. Fulton Schools of Engineering, Arizona State University, Tempe, Arizona, USA*
[2]*Institute of Chemistry, Faculty of Natural Sciences and Mathematics, Ss. Cyril and Methodius University in Skopje, Skopje, N. Macedonia*
[3]*Burge Environmental Inc., Tempe, Arizona, USA*
[4]*W. P. Carey Information Systems, W.P. Carey School of Business, Arizona State University, Tempe, USA*
[5]*Faculty of Agriculture and Food Sciences, Ss. Cyril and Methodius University in Skopje, Skopje, N. Macedonia*

kiril.hristovski@asu.edu

This study proposes a generalized model describing the temporal changes in open-circuit potentials in microbial biofilm systems. Using an Nernstian equilibrium approach combined with a series of different kinetic models for each experimental stage, it examines nutrient oxidation by microbes under anaerobic conditions with a continuous supply. New functions are derived to fit the experimental data and to provide in-depth understanding of the complex bioelectrochemical transformations occurring during the oxidation of nutrients by a biofilm.

Keywords: biofilms; open-circuit potential; thermodynamic/kinetics modeling; bioelectrochemical cells; information transfer in biofilms; charge transfer in biofilms

ПОТЕНЦИЈАЛИ ПРИ ОТВОРЕНО КОЛО КАЈ БИОФИЛМОВИ: КИНЕТИКАТА НА БИОТРАНСФОРМАЦИЈА ЈА ОДРЕДУВА ДИНАМИКАТА ПРИ АНАЕРОБНИ УСЛОВИ

Во оваа студија е предложен генерализиран модел кој ги опишува промените на потенцијалите при отворено струјно коло со текот на времето кај биофилмови изградени од микроорганизми. Користејќи рамнотежен Нернстов пристап комбиниран со серија различни кинетички модели за секоја фаза од експериментот, изучена е оксидацијата на нутриентите од страна на микроорганизмите при нивно континуирано внесување. Изведени се нови функции за фитување на експерименталните податоци и добивање продлабочени сознанија за комплексните биоелектрохемиски трансформации кои се одвиваат во текот на оксидацијата на нутриентите од страна на биофилмот.

Клучни зборови: биофилмови; потенцијал на отворено коло; термодинамичко/кинетичко моделирање; биоелектрохемиски ќелии; пренос на информации кај биофилмови; пренос на полнеж кај биофилмови

1. INTRODUCTION

Understanding the complexity of life remains a core scientific challenge,[1–5] especially due to the intricate biochemical pathways found in microbial biofilms.[6–10] An effective analysis of the communication within these consortia requires an understanding of electron transfer dynamics.[11–14]

Microbial potentiometric sensors and open-circuit potential (OCP) measurements now allow minimally invasive examination of the electrochemical properties of biofilms.[15–18] Crucially, measurement of the OCP does not disrupt intra- or intercellular processes because it does not require the flow an electrical current through the system. On the other hand, closed-circuit techniques involve externally induced electrons, which can influence biochemical processes.[19–22] The electrochemical changes measured using the OCP directly reflect biofilm biochemistry, enabling analyses of equilibrium thermodynamics.[15] Under such realistically quasi-static conditions, equilibrium thermodynamic approaches are applicable for the analysis of a range of relevant phenomena.

In heterotrophic biofilms, the change in the OCP over time can be linked to nutrient dynamics and modeled thermodynamically.[23,24] Combining Nernstian and kinetic models provides insights into OCP trends and allows one to extract key parameters underlying biochemical dynamics. Although earlier models address only simple kinetics,[23] expanded models now consider diverse kinetics and nutrient supplies. Hence, the expanded models are applicable across various systems and experimental contexts and improve understanding of kinetic variations among biofilms.[25,26] This ability can also clarify subtle kinetic differences among various biofilms.

A two-step process occurs when an equilibrated biofilm is supplied with reduced organic carbon nutrients.[23] First, nutrients enter the biofilm at a rate v. The external perturbation prompts microbial consortia to extract electrons from these nutrients (Fig. 1), oxidizing them and altering the reduced-to-oxidized concentration ratio, which shifts the OCP. During electron extraction, reduced (Red) species are converted to oxidized (Ox) species and possibly other products. The resulting OCP reflects a Nernstian equilibrium process driven by these electron and redox changes.

$$\nu_{Ox}Ox + ze^- = \nu_{Red}Red \qquad (1)$$

It is represented with a dashed line in Figure 1.

In the second step, as the input of nutrients is cut off, oxygen diffuses into the system and promotes the oxidizer reaction channel. This is reflected in a distinct trend in OCPs.

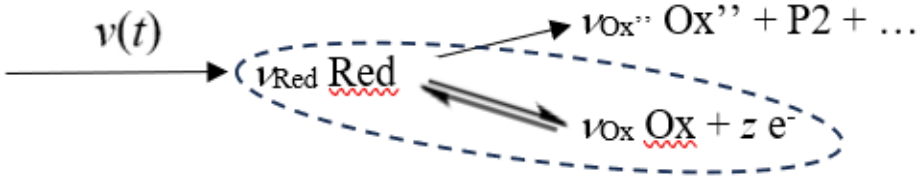

Fig. 1. A scheme of the general kinetics considered in the models.
It involves the chemical transformation pathway, supply dynamics, and Nernstian equilibrium.

In a natural system, first-order or pseudo-first-order kinetics occur most frequently. Nutrients are supplied at a constant rate, while the kinetics of their redox transformation are assumed to be linear. However, not every natural process follows first-order kinetics. Hence, it is necessary to consider a generalization of the kinetic model and to analyze the effects of kinetics on the Nernstian equilibrium governing the time dependence of OCPs. The generalization of transformation kinetics encompasses various scenarios, including n-th order or Monod oxidation kinetics, as well as non-constant nutrient supply rates. The main aims of this study are to expand the analysis of the two-step process shown in Figure 1 by examining n-th order and Monod kinetics under a constant supply and linear kinetics with a variable supply; to forecast the time dependence of OCPs for these kinetic and supply scenarios; and to develop a practical model function for fitting bioelectrochemical data from microbial biofilm systems.

2. DEVELOPMENT OF THE GENERALIZED KINETICS MODEL

2.1. *General theoretical framework*

To extend the model that describes the temporal dependence of OCPs, it is necessary to derive the equations governing the time evolution of all species illustrated in Figure 1, and to incorporate them into the Nernstian equilibrium framework. We consider three specific cases in this study: Case 1 is n-th order transformation kinetics at a constant supply rate, as a natural extension of the basic linear kinetics model. Case 2 is Monod transformation kinetics at a constant supply rate (physically, this is the most meaningful biotransformation kinetic

mode). Case 3 is linear transformation kinetics at a time-variable supply rate (providing an initial step toward the most realistic supply regime).

2.1.1. *Case 1: A constant supply rate and n-th order transformation kinetics*

In this case, the nutrient supply rate is constant (v_0) while the transformation kinetics is of the *n*-th order. In such a case, the kinetic equation for c_{Red} takes the form:

$$\frac{\mathrm{d}c_{\mathrm{Red}}}{\mathrm{d}t} = v_0 - k_n c_{\mathrm{Red}}^n \tag{2}$$

This is a separable equation, with the following general solution:

$$t + C = \int \frac{\mathrm{d}c_{\mathrm{Red}}}{v_0 - k_n \cdot c_{\mathrm{Red}}^n} \tag{3}$$

The possibility of writing the integral in (3) in a closed elementary form depends on the value of *n*. The particular solution corresponding to the initial condition $c_{\mathrm{Red}}(t = 0) = c_0$ when $n = 1$ is given by:

$$c_{\mathrm{Red}}(t) = \frac{v_{\mathrm{inp.}}}{k_1} + \left(c_0 - \frac{v_{\mathrm{inp.}}}{k_1}\right)\exp(-k_1 \cdot t) \tag{4}$$

For a trivial case of zeroth-order transformation of Red species to Ox species ($n = 0$), under the same initial conditions, the particular integral of (3) reduces to:

$$c_{\mathrm{Red}}(t) = c_0 + (v_0 - k_0) \cdot t \tag{5}$$

Extension to second-order kinetics is nontrivial. For a physically meaningful case (when both v_0 and k_2 are positive), the particular integral takes the form:

$$c_{\mathrm{Red}}(t) = \sqrt{\frac{v_0}{k_2}}\tanh\left[\sqrt{v_0 \cdot k_2} \cdot t + \operatorname{arctanh}\left(c_0\sqrt{\frac{k_2}{v_0}}\right)\right] \tag{6}$$

For the sake of a mathematically rigorous derivation, strictly speaking, solution (6) is valid for:

$$c_0 < \sqrt{\frac{v_0}{k_2}} \tag{7}$$

when

$$c_0 = \sqrt{\frac{v_0}{k_2}} \tag{8}$$

Solution (6) is a constant, that is:

$$c_{\mathrm{Red}}(t) = \sqrt{\frac{v_0}{k_2}} \tag{9}$$

On the other hand, if the condition

$$c_0 > \sqrt{\frac{v_0}{k_2}} \tag{10}$$

holds, then solution (6) has to be expressed through coth, or analytically continued. A more convenient form of solution (6), based on expansion of tanh for a sum, is the rational form:

$$c_{\mathrm{Red}}(t) = \sqrt{\frac{v_0}{k_2}} \cdot \frac{c_0\sqrt{\frac{k_2}{v_0}} + \tanh\left(\sqrt{v_0 \cdot k_2} \cdot t\right)}{1 + c_0\sqrt{\frac{k_2}{v_0}} \cdot \tanh\left(\sqrt{v_0 \cdot k_2} \cdot t\right)} \tag{11}$$

To characterize the bioelectrochemistry of the biofilm system, we follow the temporal evolution of the OCP, that is, the electromotive force (EMF) of the electrochemical element, which is composed of a biofilm electrode and an Ag|AgCl|Cl$^-$(a) electrode. As the reference electrode potential is constant, the temporal evolution of the EMF of the complete element is governed by the redox equilibrium:

$$\nu_{\mathrm{Ox}}\mathrm{Ox} + ze^- = \nu_{\mathrm{Red}}\mathrm{Red} \tag{12}$$

The Nernst equation gives the half-element potential (the cathode potential E_c):

$$E_c = E_c^{\mathrm{o}} - \frac{RT}{zF}\ln\frac{a_{\mathrm{Red}}^{\nu_{\mathrm{Red}}}}{a_{\mathrm{Ox}}^{\nu_{\mathrm{Ox}}}} \tag{13}$$

with a_{Red} and a_{Ox} being the relative activities of Red and Ox species, respectively. Subsequently, the measured EMF (*i.e.*, the OCP) is given by the difference between the cathode and anode potentials (E_a):

$$\Delta E = E = E_c - E_a = E_c^{\mathrm{o}} - \frac{RT}{zF}\ln\frac{c_{\mathrm{Red}}^{\nu_{\mathrm{Red}}}}{c_{\mathrm{Ox}}^{\nu_{\mathrm{Ox}}}} - E_a^{\mathrm{o}} \tag{14}$$

Specifically:

$$E = (E_c^{\mathrm{o}} - E_a^{\mathrm{o}}) - \frac{RT}{zF}\ln\frac{c_{\mathrm{Red}}^{\nu_{\mathrm{Red}}}}{c_{\mathrm{Ox}}^{\nu_{\mathrm{Ox}}}} \tag{15}$$

As the Ox species involved in the redox equilibrium determining the EMF are not formed directly from the Red species, the time dependence of E is governed by the temporal evolution of $c_{\mathrm{Red}}(t)$:

$$E(t) = (E_c^{\mathrm{o}} - E_a^{\mathrm{o}}) - \frac{RT}{zF}\ln\frac{[c_{\mathrm{Red}}(t)]^{\nu_{\mathrm{Red}}}}{c_{\mathrm{Ox}}^{\nu_{\mathrm{Ox}}}} \tag{16}$$

Substituting (11) in (16) and performing an algebraic transformation, we arrive at:

$$E(t) = (E_c^o - E_a^o) + \frac{RTv_{\mathrm{Ox}}}{zF}\ln c_{\mathrm{Ox}} - \frac{RTv_{\mathrm{Red}}}{zF}\ln\left[\sqrt{\frac{v_0}{k_2}}\cdot\frac{c_0\sqrt{\frac{k_2}{v_0}}+\tanh\left(\sqrt{v_0\cdot k_2}\cdot t\right)}{1+c_0\sqrt{\frac{k_2}{v_0}}\cdot\tanh\left(\sqrt{v_0\cdot k_2}\cdot t\right)}\right] \quad (17)$$

Figure 2 shows a plot of the $E(t)$ dependence governed by function (17), compared with the corresponding dependence when the Red species transforms according to linear kinetics, for a particular choice of parameters c_0, k_2, and v_0. It can be seen that second-order kinetics leads to a slower decay in the OCP as compared with the linear case. Therefore, in principle the rate of change of $E(t)$ can be used to deduce the transformation kinetics of the nutrient species.

It is interesting to note that a specific case when n = 1/2 is also analytically solvable, and the temporal evolution of c_{Red} may be expressed through the Lambert W function:[27]

$$c_{\mathrm{Red}}(t) = \left(\frac{v_0}{k_{1/2}}\right)^2\cdot\left[1 + W\left(-\frac{\exp\left(-1-\frac{k_{1/2}^2}{2v_0}\cdot t-\frac{k_{1/2}}{v_0}\sqrt{c_0}\right)}{v_0\cdot\left(v_0-k_{1/2}\sqrt{c_0}\right)}\right)\right]^2 \quad (18)$$

In such a case, $E(t)$ takes the following form:

$$E(t) = (E_c^o - E_a^o) + \frac{RTv_{\mathrm{Ox}}}{zF}\ln c_{\mathrm{Ox}} - \frac{2RTv_{\mathrm{Red}}}{zF}\ln\left\{\left(\frac{v_0}{k_{1/2}}\right)\cdot\left[1 + W\left(-\frac{\exp\left(-1-\frac{k_{1/2}^2}{2v_0}\cdot t-\frac{k_{1/2}}{v_0}\sqrt{c_0}\right)}{v_0\cdot\left(v_0-k_{1/2}\sqrt{c_0}\right)}\right)\right]\right\} \quad (19)$$

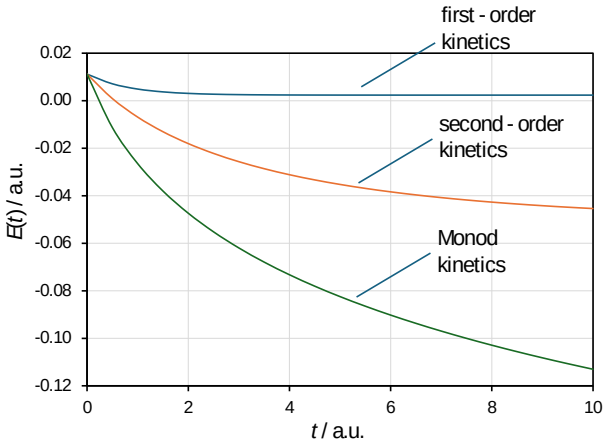

Fig. 2. A plot of the temporal dependence of the open-circuit potential $E(t)$ in cases of different kinetics of the upper channel in Fig. 1, for a particular choice of the parameters c_0, k_2, and v_0 (a.u. – arbitrary units).

2.1.2. *Case 2: A constant supply rate and Monod transformation kinetics*

In biofilm growth kinetics, as well as in more general cases of microbial growth studies, the Monod scheme is often assumed to realistically describe the kinetics of microbial growth processes.[28] Using this transformation kinetic scheme, with respect to the Red species in our case, the following kinetic equation holds:

$$\frac{\mathrm{d}c_{\mathrm{Red}}}{\mathrm{d}t} = v_0 - \frac{k_{\max}c_{\mathrm{Red}}}{k_M + c_{\mathrm{Red}}} \quad (20)$$

The two special cases corresponding to $k_{\mathrm{M}} >> c_{\mathrm{Red}}$ and $k_{\mathrm{M}} << c_{\mathrm{Red}}$ give first-order decomposition kinetics (as well as the constant supply rate v_0), which we analyzed in detail in our previous study,[23] and zeroth-order decomposition kinetics, respectively. Solution of differential equation (20), with the initial condition $c_{\mathrm{Red}}(t = 0) = c_0$, depends on the v_0 *versus* $k_{\max}$ ratio. In a general case, when $v_0 \neq k_{\max}$, the equation can be solved so that the function is obtained in an implicit form (see the Supporting Information for a detailed solution algorithm):

$$\frac{c_{\mathrm{Red}}(t)}{v_0 - k_{\max}} - \frac{k_{\max}k_M}{(v_0 - k_{\max})^2}\ln[v_0k_M + (v_0 - k_{\max})\cdot c_{\mathrm{Red}}(t)] =$$

$$= t + \frac{c_0}{v_0 - k_{\max}} - \frac{k_{\max}k_M}{(v_0 - k_{\max})^2}\ln[v_0k_M + (v_0 - k_{\max})\cdot c_0] \quad (21)$$

To the best of our knowledge, it does not seem to be possible to express the solution in an explicit form using elementary functions. However, it is possible to numerically solve (21) for a given set of parameters (and the choice of a physically meaningful branch consistent with the initial conditions). The corresponding time evolution of E:

$$E(t) = (E_c^o - E_a^o) + \frac{RTv_{\mathrm{Ox}}}{zF}\ln c_{\mathrm{Ox}} - \frac{RTv_{\mathrm{Red}}}{zF}\ln[c_{\mathrm{Red}}(t)] \quad (22)$$

is presented in Figure 2.

2.1.3. *Case 3: A time-dependent supply rate and first-order transformation kinetics*

Cases 1 and 2 assume a constant supply rate of nutrients. A more realistic scenario involves a

time-dependent supply rate. We first consider an exponentially decaying supply rate given by:

$$v = v_0 \exp(-kt) \qquad (23)$$

With a function of this form, the kinetic equation in (2) takes the form:

$$\frac{\mathrm{d}c_{\mathrm{Red}}}{\mathrm{d}t} = v_0 \exp(-kt) - k_1 c_{\mathrm{Red}} \qquad (24)$$

This linear first-order differential equation has an integrating factor:

$$\mu(t) = \exp(\int k_1 t \mathrm{d}t) = \exp(k_1 t) \qquad (25)$$

The particular solution for the initial condition $c_{\mathrm{Red}}(t = 0) = c_0$ has the form:

$$c_{\mathrm{Red}}(t) = \frac{v_0}{k_1 - k}\exp(-kt) + \left(c_0 - \frac{v_0}{k_1 - k}\right)\exp(-k_1 t) \qquad (26)$$

In a specific case, when $k = k_1$, it reduces to the form:

$$c_{\mathrm{Red}}(t) = (v_0 t + c_0)\exp(-kt) \qquad (27)$$

For the generalized case ($k \neq k_1$), $E(t)$ takes the form:

$$E(t) = (E_c^{\mathrm{o}} - E_a^{\mathrm{o}}) + \frac{RTv_{\mathrm{Ox}}}{zF}\ln c_{\mathrm{Ox}} - \frac{RTv_{\mathrm{Red}}}{zF} \cdot$$
$$\cdot \ln\left[\frac{v_0}{k_1 - k}\exp(-kt) + \left(c_0 - \frac{v_0}{k_1 - k}\right)\exp(-k_1 t)\right] \qquad (28)$$

Figure 3 compares the time-dependencies of E given by (28) for different values of the k/k_1 ratio with the corresponding dependencies in the case of a constant supply rate, given by:

$$E(t) = (E_c^{\mathrm{o}} - E_a^{\mathrm{o}}) + \frac{RTv_{\mathrm{Ox}}}{zF}\ln c_{\mathrm{Ox}} -$$
$$-\frac{RTv_{\mathrm{Red}}}{zF}\ln\left\{\frac{v_0}{k_1} + \left(c_0 - \frac{v_0}{k_1}\right)\cdot \exp(-k_1 \cdot t)\right\} \qquad (29)$$

Therefore, the time dependence of v can be accounted for and used to fine-tune the model, allowing for an even more accurate description of the temporal evolution of the OCPs.

Other types of reaction kinetics in this context (such as Monod kinetics, generalized n-th order kinetics, or fractional kinetics) do not allow for analytical solutions of the overall kinetic equations. Although such cases are certainly of interest, the lack of analytical solutions limits their applicability in the context of, for example, fitting to experimental data.

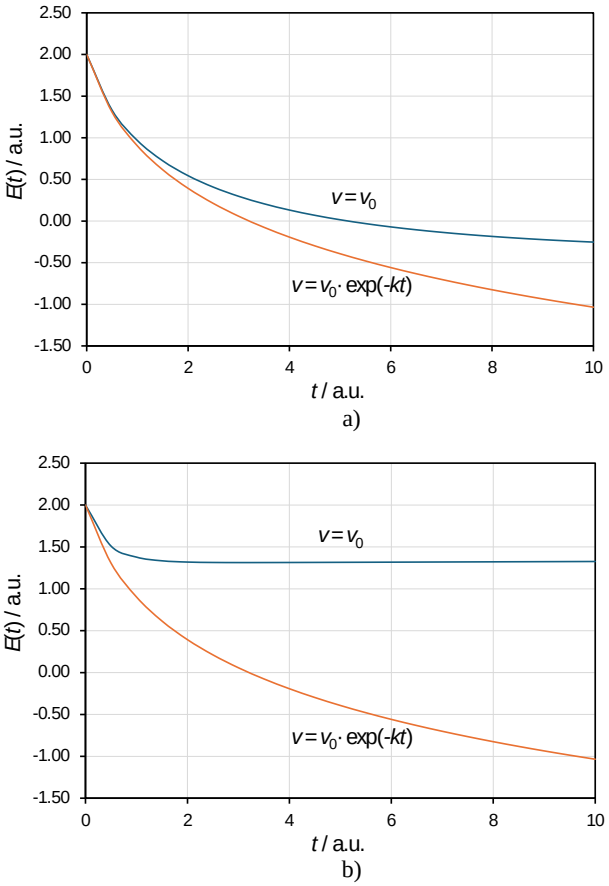

Fig. 3. Temporal dependence of the open-circuit potential E in the case of time-dependent and constant nutrient supply rates when the k/k_1 ratio is a) 10^{-2} and b) $k/k_1 = 10^{-3}$ (a.u. – arbitrary units).

3. CONCLUSIONS

This study extends our recent model, which integrates Nernstian thermodynamics with kinetics to analyze the temporal dynamics of OCPs in biofilm systems. We specifically examine anaerobic oxidation under a continuous nutrient supply, considering scenarios of constant and time-varying nutrient transformation rates by the biofilm's microbial consortium. Our model accommodates various real-world conditions, enhances our understanding of electrochemical behavior in these systems, and explains the observed changes in OCPs. Additionally, the updated approach improves modularity and enables the inclusion of environmental effects. The new model functions can fit *in situ* experimental data and yield additional insights into biofilm biochemical kinetics.

REFERENCES

(1) Gomez-Marquez, J. What is life? *Mol. Biol. Rep.* **2021**, *48*, 6223–6230.

(2) Witzany, G. What is life? *Front. Astron. Space Sci.* **2020**, *18*, 7 (1–13).

(3) Elani, Y.; Seddon, J. M. What it means to be alive: a synthetic cell perspective. *Interface Focus* **2023**, *13*, 20230036 (1–3).

(4) Otto, S. An approach to the de novo synthesis of life. *Acc. Chem. Res.* **2022**, *55*, 145–155.

(5) Vitas, M.; Dobovisek, A. Towards a general definition of life. *Discover Life* **2019**, *49*, 77–88.

(6) *Fundamentals of Biofilm Research;* Lewandowski, Z., Beyenal, H.; CRC Press: Boca Raton, 2007.

(7) Sauer, K.; Stoodley, P.; Goeres, D. M.; Hall-Stoodley, L.; Burmølle, M.; Steward, P. S.; Bjarnsholt, T. The biofilm life cycle: expanding the conceptual model of biofilm formation. *Nat. Rev. Microbiology* **2022**, *20*, 608-620.

(8) Flemming, H-C.; Van Hullebuch, E. D.; Neu, T. R.; Nielsen, P. H.; Seviour, T.; Stoodley, P.; Wingender, J.; Wuertz, S. The biofilm matrix: multitasking in a shared space. *Nat. Rev. Microbiology* **2022**, *21*, 70–86.

(9) Penesyan, A.; Paulsen, I. T.; Kjelleberg, S.; Gillings, M. R. Three faces of biofilms: a microbial lifestyle, a nascent multicellular organism, and an incubator for diversity. *NPJ Biofilms and Microbiomes* **2021**, *7*, 80 (1–9).

(10) Donlan, R. M. Biofilms: Microbial life on surfaces. *Emerg. Infect. Dis.* **2002**, *8*, 881–890.

(11) De Lichtervelde, A. C. L.; ter Heijne, A.; Hamelers, H. V. M.; Biesheuvel, P. M.; Dykstra, J. E. Theory of ion and electron transport coupled with biochemical conversions in an electroactive film. *Phys. Rev. Applied* **2019**, 12, 014018 (1–11).

(12) Philips, J.; Verbeeck, K.; Rabaey, K.; Arends, J. B. A. Electron transfer in biofilms. In: *Microbial Electrochemical and Fuel Cells*; Elsevier: Amsterdam, 2016; pp. 67–113.

(13) Manna, S.; Ghanty, C.; Baindara, P.; Barik, T. Kr.; Mandal, S. M. Electrochemical communication in biofilm of bacterial community. *J. Basic Microbiol.* **2020**, *60*, 819–827.

(14) Prindle, A.; Liu, J.; Asally, M.; Ly, S.; Garcia-Ojalvo, J.; Süel, G. M. Ion channels enable electrical communication in bacterial communities. *Nature* **2015**, *527*, 59–63.

(15) Burge, S. R.; Hristovski, K. D.; Burge, R. G.; Pejov, Lj.; Boscovic, D.; Taylor, E.; Hoffman, D. A. Exploring the electrical nature of biofilms for long-term monitoring of quiescent aquatic environments via open-circuit microbial potentiometric sensors: Evidence of long-distance electrical signaling. *Nano Life* **2023**, *13*, 2350014 (1–13).

(16) Burge, S. R.; Hristovski, K. D.; Burge, R. G.; Saboe, D.; Hoffman, D. A.; Koenigsberg, S. S. Microbial potentiometric sensor array measurements in unsaturated soils. *Sci. Total Environ.* **2021**, *751*, 142342 (1–7).

(17) Sale, T.; Gallo, S.; Askarani, K. K.; Irianni-Renno, M.; Lyverse, M.; Hopkins, H.; Blotevogel, J.; Burge, S. Real-time soil and groundwater monitoring via spatial and temporal resolution of biogeochemical potentials. *J. Hazard. Mater.* **2021**, *408*, 124403 (1–11).

(18) Brown, F. C.; Burge, S. R.; Hristovski, K. D.; Burge, R. G.; Taylor, E.; Hoffman, D. A. Microbial potentiometric sensor technology for real-time detection and monitoring of toxic metals in aquatic matrices. *Maced. J. Chem. Chem. Eng.* **2020**, *39*, 119–127.

(19) Burge, S. R.; Hristovski, K. D.; Burge, R. G.; Hoffman, D. A.; Saboe, D.; Chao, P.; Taylor, E.; Koenigsberg, S. S. Microbial potentiometric sensor: A new approach to longstanding challenges. *Sci. Total Environ.* **2020**, *742*, 140528 (1–12).

(20) Saboe, D.; Ghasemi, H.; Gao, M. M.; Samardzic, M.; Hristovski, K. D.; Boscovic, D.; Burge, S. R.; Burge, R. G.; Hoffman, D. A. Real-time monitoring and prediction of water quality parameters and algae concentrations using microbial potentiometric sensor signals and machine learning tools. *Sci. Total Environ.* **2021**, *764*, 142876 (1–8).

(21) Saboe, D.; Hristovski, K. D.; Burge, S. R.; Burge, R. G.; Taylor, E.; Hoffman, D. A. Measurement of free chlorine levels in water using potentiometric responses of biofilms and applications for monitoring and managing the quality of potable water. *Sci. Total Environ.* **2021**, *766*, 144424 (1–7).

(22) Hristovski, K. D.; Burge, S. R.; Boscovic, D.; Burge, R. G.; Babanovska-Milenkovska, F. Real-time monitoring of kefir-facilitated milk fermentation using microbial potentiometric sensors. *J. Environ. Chem. Eng.* **2022**, *10*, 107491 (1–8).

(23) Pejov, L.; Hristovski, K. D.; Burge, S. R.; Burge, R. G.; Boscovic, D. Temporal dynamics of the biofilm-mediated open circuit potentials: Understanding the fundamentals via a combined thermodynamic and kinetic modeling approach. *Biointerphases* **2025**, *20*, 011005 (1–11).

(24) Burge, S. R.; Hristovski, K. D.; Pejov, L.; Burge, R. G.; Hoffman, D.; Boscovic, D.; Harding, R. Nature's first electrical tool: microbial biofilms using electron transfer networks to perform aerobic respiration in an anaerobic environment. *Bioelectrochemistry* **2026**, *167*, 109076.

(25) Almquist, J.; Cvijovic, M.; Hatzimanikatis, V.; Nielsen, J.; Jirstrand, M. Kinetic models in industrial biotechnology – Improving cell factory performance. *Metabol. Eng.* **2014**, *24*, 38–60.

(26) Amin, M. S. A.; Mozumder, Md. S. I.; Stubert, F.; Giralt, J.; Fortuny, A.; Fabregat, A.; Font, J. Biofilm model development and process analysis of anaerobic biodegradation of azo dyes, *Environ. Technol. & Innov.* **2023**, *29*, 102962 (1–15).

(27) Loczi, L. Guaranteed- and high-precision evaluation of the Lambert W function. *Appl. Math. Comput.* **2022**, *433*, 127406 (1–22).

(28) Spormann, A. M., *Microbial Kinetics. Principles of Microbial Metabolism and Metabolic Ecology*. Springer: Cham, 2023.